

AN OPTIMIZATION METHOD FOR AUTOREGRESSIVE TIME SERIES FORECASTING

A PREPRINT

Zheng Li, Jerry Cheng, Huanying Gu

Department of Computer Science, New York Institute of Technology, New York, NY 10023
 zli66@nyit.edu, jcheng18@nyit.edu, hgu03@nyit.edu

February 3, 2026

ABSTRACT

Current time-series forecasting models are primarily based on transformer-style neural networks. These models achieve long-term forecasting mainly by scaling up the model size rather than through genuinely autoregressive (AR) rollout. From the perspective of large language model training, the traditional training process for time-series forecasting models ignores temporal causality. In this paper, we propose a novel training method for time-series forecasting that enforces two key properties: (1) AR prediction errors should increase with the forecasting horizon. Any violation of this principle is considered random guessing and is explicitly penalized in the loss function, and (2) the method enables models to concatenate short-term AR predictions for forming flexible long-term forecasts. Empirical results demonstrate that our method establishes a new state-of-the-art across multiple benchmarks, achieving an MSE reduction of more than 10% compared to *iTransformer* and other recent strong baselines. Furthermore, it enables short-horizon forecasting models to perform reliable long-term predictions at horizons over 7.5 times longer. Code is available at <https://github.com/LizhengMathAi/AROpt>

Keywords optimization · loss function · autoregressive model · time-series forecasting · long-term prediction

1 Introduction

Transformer-based architectures have emerged as the dominant paradigm in time-series forecasting, having demonstrated excellent performance across diverse benchmarks. A key milestone was PatchTST [Nie, 2022], inspired by ViT [Dosovitskiy, 2020], which segments each univariate time series into subseries-level patches. Building on this, *iTransformer* [Liu et al., 2023] introduced an inverted design: instead of tokenizing along the temporal dimension, it treats variates as tokens. This approach has achieved state-of-the-art (SOTA) results in long-term forecasting, addressing limitations of prior temporal-token Transformers and outperforming them on many benchmarks.

Currently, time-series forecasting models typically handle varying forecast horizons by scaling model size or complexity [Nie, 2022, Wu et al., 2022, Zhou et al., 2021, Huang

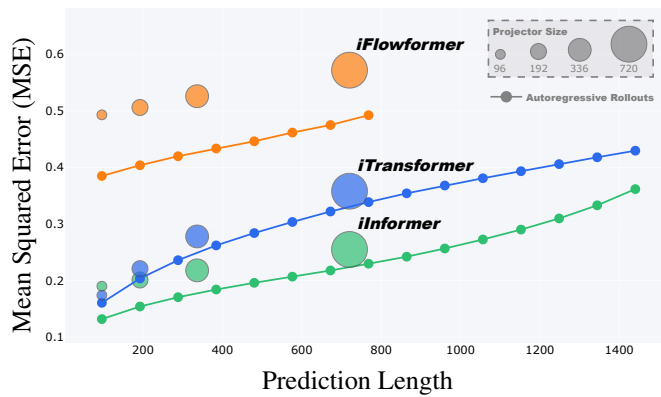


Figure 1: **Specialized long-horizon forecasting models (vanilla training) vs. single short-horizon forecasting model (trained with our method and inferred in AR rollout mode).** *iTransformer* (Weather), *iInformer* (Traffic), *iFlowformer* (Electricity). Our method outperforms vanilla training on short horizons. Enable small models to output arbitrary-length forecasts via AR rollouts without retraining, and surpass larger, specialized models on long-horizon forecasting.

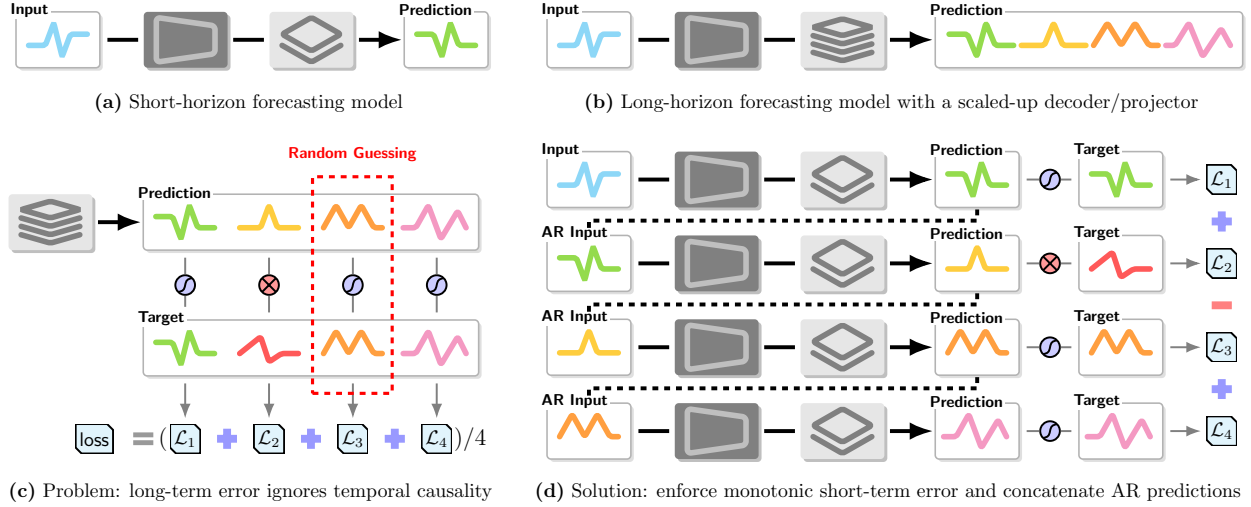


Figure 2: **Direct long-term forecasting vs. AR rollout forecasting** (a) A short-horizon forecasting model that predicts the next forecasting horizon using an encoder–projector architecture. This architecture is based solely on iTraformer, and the output window is strictly separated from the input window. In contrast, for Informer, Flashformer, and Flowformer, the projector is contained within the decoder, and they employ overlapping input–output windows. (b) A long-horizon forecasting model that reuses the same encoder but scales up the decoder/projector to directly predict longer future horizons. (c) Problem: direct long-horizon forecasting ignores temporal causality, which can lead to random guessing – early predictions exhibit larger errors, whereas later predictions do not accumulate errors and instead produce smaller errors, potentially due to chance. (d) We propose a new loss function that enforces temporal causality: short-term AR rollout predictions should exhibit increasing error \mathcal{L}_t as the time step t increases. Violations of this constraint indicate random guessing and are penalized in the total loss. These short-term AR rollout predictions are then concatenated to form long-horizon predictions.

et al., 2022, Dao et al., 2022, Liu et al., 2023]. This design inherently limits their ability to perform any-length forecasting, rendering them inflexible for diverse industrial applications. In contrast, causal language modeling (e.g., GPT [Radford et al., 2018]) and generative vision models address similar challenges through AR rollout. For example, in the era of large language models (LLMs), GPT generates text of arbitrary length by iteratively: it predicting the next token conditioned on all previous tokens. This capability is crucial, as it enables a single model to support diverse output lengths without the need for retraining or horizon-specific architectural modifications. However, directly applying the same AR rollout idea to time-series forecasting often yields poor performance in practice [Marcellino et al., 2006, Box et al., 2015]. This is primarily driven by the accumulated error problem: unlike language models, time-series models are not focused on classification tasks. As a result, small prediction errors at early steps propagate and accumulate during long-horizon rollout, leading to rapid degradation in forecast quality [Marcellino et al., 2006].

Temporal causality has become an efficient mechanism for improving model performance; DeepSeek-V3 [Liu et al., 2024] first introduced a similar idea as a refined form of Multi-Token Prediction [Gloeckle et al., 2024]. Unlike reinforcement learning (RL) methods commonly used in language model post-training, DeepSeek-V3 adopts an additional selective approach to discard certain predictions during inference. This idea has demonstrated broad utility across computer vision, semantic segmentation, and complex reasoning tasks [Li et al., 2025].

In this work, we propose an optimization method for time-series forecasting. As shown in Fig. 2(a & b), current models require scaling model size to handle varying-length predictions. However, long-term errors may not obey temporal causality (Fig. 2(c)). We address this problem by collecting AR rollout errors and incorporating a new penalty term into the loss function (Fig. 2(d)). Our method enables forecasting models to produce high-quality outputs at any length and achieves an MSE reduction of more than 10% compared to iTraformer and other recent strong baselines.

This paper is organized as follows. Section 2 reviews related work on temporal causality, AR rollouts, multi-token prediction, and zero-shot generation. Section 3 introduces our proposed algorithm, including our AR rollout pipeline and the novel loss function constructed with RL-style rewards. Section 4 provides a convergence analysis of the proposed loss function. Section 5 presents experimental results, including setup details, contribution of short-term

Algorithm 1 AR rollout objective function and concatenating short-term prediction for long-horizon forecasting. Given historical context length S , rollout stride T , input–output overlap length L (for iTransformer-style architectures, $L = 0$), and number of rollout steps n . Let $\gamma \in (0, 1)$ be the decay factor (default: 0.5) and $\beta \in (0, 0.5)$ the smoothing weight (default: 0.1). $f(\cdot; \theta)$ denotes the inference function and \mathcal{L} the loss function (default: MSE). $\text{sg}(\cdot)$ denotes the stop-gradient operator.

- 1: **Input:** Historical context and future ground-truth sequence $\mathbf{X} = \{x_0, \dots, x_{S+nT-1}\}$
- 2: $\hat{\mathbf{X}}_{:S} \leftarrow \mathbf{X}_{:S}$ (Pad the prediction sequence)
- 3: $\hat{\mathbf{X}}_{S:S+T} \leftarrow f(\mathbf{X}_{:S}; \theta)_{L:L+T}$ (Generate the first prediction block for AR rollout)
- 4: $e_1 \leftarrow \mathcal{L}(\hat{\mathbf{X}}_{S:S+T}, \mathbf{X}_{S:S+T})$ (Compute the loss of the first prediction block)
- 5: $\ell \leftarrow e_1$
- 6: **for** $k \leftarrow 1$ **to** $n - 1$ **do**
- 7: $\hat{\mathbf{X}}_{S+kT:S+(k+1)T} \leftarrow f(\hat{\mathbf{X}}_{kT:S+kT}; \theta)_{L:L+T}$ (Generate the $(k + 1)$ -th prediction block autoregressively)
- 8: $e_{k+1} \leftarrow \mathcal{L}(\hat{\mathbf{X}}_{S+kT:S+(k+1)T}, \mathbf{X}_{S+kT:S+(k+1)T})$ (Compute the loss of the $(k + 1)$ -th prediction block)
- 9: $\ell \leftarrow \ell + \gamma^k((1 - \beta)e_{k+1} + \beta|e_{k+1} - \text{sg}(e_k)|)$ (Accumulate the discounted loss with smoothing penalty)
- 10: **end for**
- 11: **Return:** objective function ℓ and the long-term prediction $\hat{\mathbf{X}}_{S-L:S+nT} = \{\hat{x}_{S-L}, \dots, \hat{x}_{S+nT-1}\}$

improvements, and our findings on SOTA model ranking reversal and error accumulation in AR rollouts. Section 6 discusses future work, and Section 7 concludes the paper.

2 Related Work

2.1 Temporal Causality in Forecasting Models

Current high-performance sequential models for time series forecasting are typically based on the Transformer architecture. Traditionally, these forecasters employ an encoder-decoder structure as their core architecture with the same input/output data format as in standard Transformer training, where the input sequence and target sequence share an overlapping subsequence [Wu et al., 2021, Nie, 2022, Zhou et al., 2022]. In contrast, iTransformer introduces a major conceptual shift and achieves significantly stronger baseline performance [Liu et al., 2023]: its predictions strictly begin at the time location after the input sequence (with no overlapping window). This design raises confusion, as it appears to suggest that temporal causality is unimportant. In Section 5.2.3, we demonstrate that respecting temporal causality remains crucial in model training. By enforcing monotonic error, our approach enables AR rollouts that support predictions at least $14\times$ longer than those of conventional methods, effectively paving the way for near-infinite-horizon forecasting.

2.2 Autoregressive Rollout

Autoregressive rollout is a model inference pipeline that is widely used in language models [Vaswani et al., 2017, Radford et al., 2019]. By using the model predictions as subsequent inputs, a model can iteratively generate sequences of arbitrary length. This enables the model to generate infinite-length content. However, this approach does not work in time series forecasting due to two issues: (1) outputs are continuous values, in contrast to the inherent discrete nature of causal language modeling [Zhou et al., 2021, Wu et al., 2021], and (2) AR prediction errors increase with the forecasting horizon. Even a small error can alter the future trajectory, as errors accumulate rapidly [Marcellino et al., 2006]. Inspired by the accept/reject mechanism from DeepSeek-V3 pre-training, we propose a model training framework that successfully mitigates these instabilities, enabling robust AR rollout for forecasting.

2.3 Multi-Token Prediction

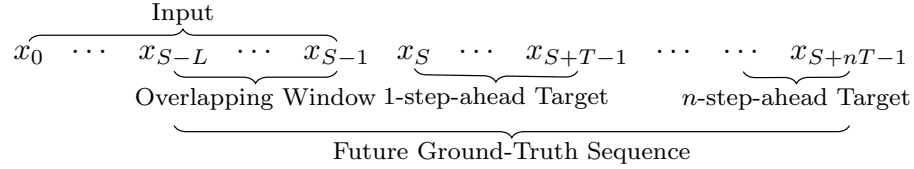
The raw multi-token prediction serves as an auxiliary objective in language models, duplicating the model head to predict multiple future tokens in a single forward pass [Gloeckle et al., 2024]. However, this approach often shows no significant improvement in model performance. In the DeepSeek-V3 technical report, the authors reformulate this concept by using a shared-head structure to prevent excessive parameter scaling, then incorporate temporal causality into multi-token prediction to selectively accept or reject the additional outputs [Liu et al., 2024]. In Section 3, we extend this accept/reject mechanism by integrating it with AR rollout. Notably, our approach requires no architectural modifications; instead, we embed this causal mechanism directly into the objective loss function.

2.4 Zero-shot Generation

Zero-shot generation enables models to generalize to new tasks without requiring task-specific retraining or fine-tuning [Sanh et al., 2021]. While this capability has been popularized through in-context learning in language and generative vision models [Radford et al., 2021, Tian et al., 2024], its potential in time-series forecasting remains a critical research area. These advances provide substantial inspiration for research in time-series forecasting. Traditional forecasting models typically require the target sequences to match the length of the model projector and predicted sequences. This rigidity imposes significant bottlenecks: longer prediction horizons make constraints on small datasets and increase computational costs during training. In contrast, models optimized for zero-shot generation overcome this restriction. For example, a model trained on short prediction horizons (e.g., 96 steps) can reliably make long-horizon forecasting (e.g., 720 steps) via AR rollout at inference time. In Section 5.2.3, we demonstrate that our method achieves this capability.

3 Algorithm

See Algorithm 1 for the pseudocode of our proposed method. Let $f(\cdot; \theta) : \mathbb{R}^S \mapsto \mathbb{R}^{L+T}$ denote the model inference function with parameters θ , where the input is a sequence with length S , the target has length $L + T$, and L is the overlap length. We are interested in extending this mapping to $\mathbb{R}^S \mapsto \mathbb{R}^{L+nT}$ via n -step AR rollout. This extension aligns the model with the following input-output or input-target structure:



Let $\{\hat{x}_{S-L}, \dots, \hat{x}_{S+nT-1}\}$ denote the final expected long-term predictions, initialized as:

$$(\hat{x}_{S-L}, \dots, \hat{x}_{S+T-1}) = f(x_0, \dots, x_{S-1}; \theta). \quad (1)$$

We then use the last S elements from the k -step prediction block as input to perform the $(k+1)$ -step prediction block:

$$(\hat{x}_{S+kT-L}, \dots, \hat{x}_{S+(k+1)T-1}) = f(\hat{x}_{kT}, \dots, \hat{x}_{S+kT-1}; \theta). \quad (2)$$

Subsequently, we repeat this AR rollout step until the prediction sequence of length $L + nT$ is fully filled.

Due to a common principle in time-series forecasting which states that **small errors in early predictions can alter the future trajectory and lead to Accumulated Prediction Error (APE) over time** [Box et al., 2015], we consider incorporating the temporal causality into the minimization of the traditional MSE loss:

$$\min_{\theta} \frac{1}{n} \sum_{t=S}^{S+nT-1} |x_t - \hat{x}_t|^2 \quad (3a)$$

$$\text{subject to } |x_t - \hat{x}_t| \geq |x_{t-1} - \hat{x}_{t-1}|, \forall t. \quad (3b)$$

Because the mini-batch training strategy renders the MSE loss a stochastic scalar function, traditional constrained optimization methods, such as the Lagrange multiplier method and barrier methods [Boyd and Vandenberghe, 2004], are not applicable here. To address this issue, we introduce an RL-style reward function that encourages the model to generate outputs satisfying the **temporal monotonicity condition** (Eq. 3b) during training. At the k -th step of the AR rollout, the MSE is taken over the entire prediction block:

$$e_k = \frac{1}{T} \sum_{t=S+kT}^{S+(k+1)T-1} |x_k - \hat{x}_k|^2.$$

To encourage the model predictions for satisfying the temporal monotonicity condition (Eq. 3b), we define the following reward function to increase its value whenever this condition is met:

$$r_k \triangleq \begin{cases} e_0 & \text{if } k = 0, \\ -(1 - \beta)e_k - \beta|e_k - \text{sg}(e_{k-1})| & \text{if } k > 1. \end{cases} \quad (4)$$

The hyperparameter $\beta \in (0, 0.5)$ controls the weight of the penalty term, while $\text{sg}(\cdot)$ denotes the stop-gradient operator, which acts as the identity function during the forward pass but prevents gradient computation through backpropagation [Chen and He, 2021]. In this case, the gradient norm of the reward decreases upon detecting random guessing:

$$\nabla_{\theta} r_k = \begin{cases} -\nabla_{\theta} e_k & \text{if } e_k > e_{k-1}, \\ -(1 - \beta)\nabla_{\theta} e_k & \text{if } e_k = e_{k-1}, \\ -(1 - 2\beta)\nabla_{\theta} e_k & \text{if } e_k < e_{k-1}. \end{cases}$$

The above equation describes our RL-style policy: model parameter updates are prevented if random guessing is detected, and facilitated if the temporal monotonicity condition (Eq. 3b) is satisfied.

Finally, we set the objective loss as the negative of a discounted return with factor γ , in the spirit of the policy gradient method [Sutton et al., 1999]:

$$\ell \triangleq -\sum_{k=0}^{n-1} \gamma^k r_k. \quad (5)$$

γ is fixed to be 0.5. The reason is that when the per-step errors e_k increase monotonically but remain of comparable magnitude, the effective accumulated loss is given by

$$\ell = \frac{1 - \gamma^n}{1 - \gamma} \mathcal{O}(e_0) \approx 2\mathcal{O}(e_0) \quad (6)$$

for large n . Thus, the objective has roughly twice the magnitude of a conventional MSE in short-term prediction. Empirically, we find that $\beta = 0.1$ yields substantial performance improvements across diverse baseline models.

4 Convergence Analysis

We provide a qualitative, semi-formal analysis of convergence behavior by comparing our loss function with the MSE loss.

Assume the error e_k of the k -step prediction block has bounded gradient norm $\mathbb{E}[\|\nabla_{\theta} e_k\|] \leq d$, we define the centered noise for the gradient of reward function:

$$G_k := \nabla_{\theta} r_k - \mathbb{E}[\nabla_{\theta} r_k].$$

Then the centered gradient estimator is

$$\nabla_{\theta} \ell - \mathbb{E}[\nabla_{\theta} \ell] = -\sum_{k=0}^{n-1} \gamma^k G_k. \quad (7)$$

By the Cauchy–Schwarz inequality,

$$\mathbb{E} \left[\left\| \sum_{k=0}^{n-1} \gamma^k G_k \right\|^2 \right] \leq \left(\sum_{k=0}^{n-1} \gamma^k \sqrt{\mathbb{E}[\|G_k\|^2]} \right)^2. \quad (8)$$

From the definition (4),

$$\|\nabla_{\theta} r_k\| \leq \|\nabla_{\theta} e_k\|$$

Thus,

$$\mathbb{E}[\|G_k\|^2] \leq \mathbb{E}[\|\nabla_\theta r_k\|^2] \leq \mathbb{E}[\|\nabla_\theta e_k\|^2] \leq d^2. \quad (9)$$

Substituting the inequalities (7), (8), and (9), we obtain the bound of the gradient norm

$$\mathbb{E}[\|\nabla_\theta \ell\|^2] = \mathbb{E}\left[\left\|\sum_{k=0}^{n-1} \gamma^k G_k\right\|^2\right] \leq \left(\sum_{k=0}^{n-1} \gamma^k d\right)^2 < 4d^2.$$

This estimation guarantees that our loss converges during training whenever the standard MSE loss converges.

5 Experiments

Our proposed approach is model-agnostic and applies to SOTA models (iTransformer and its variants) without altering the core architecture. Specifically, its optimization method operates on a novel loss function and data pipeline to enable AR rollouts for varying-length predictions across multivariate time-series forecasting benchmarks. Experiments demonstrate that our method not only enhances model performance for short-term forecasting but also enables short-horizon forecasting models to generate high-accuracy long-term predictions via AR rollouts, often outperforming models specifically scaled for longer-term forecasting. All experiments are designed to be fully reproducible.

5.1 Setup

We adopt the widely used benchmarks from the iTransformer study [Liu et al., 2023], including Exchange, Electricity (ECL), Traffic, Weather, Solar-Energy, and PEMS. These datasets capture diverse real-world scenarios: Exchange consists of daily exchange rates for eight countries; Electricity records hourly power consumption across 321 clients; Traffic measures hourly road occupancy from 862 San Francisco Bay area highway sensors (2015–2016); Weather tracks 21 meteorological variables at 10-minute intervals in Germany (2020); Solar-Energy monitors the solar power production from 137 PV plants in 2006; and PEMS datasets reflect traffic flow across the California state highway system.

Since iTransformer and its variants already achieve SOTA results on standard benchmarks, we primarily apply our proposed method to four inverted Transformer architectures: iTransformer, iInformer, iFlowformer, and iFlashformer. Baseline numbers are taken directly from that work, where each model is trained independently for every prediction length. For ablation studies, we adopt the same Adam optimizer and relevant configurations as in that work; experiments run on a single NVIDIA RTX A6000 GPU.

Our approach introduces three additional hyperparameters: the reward discount factor γ , the penalty weight β , and the number of AR rollout steps n . We intentionally fix these hyperparameters (see the default settings in Algorithm 1) across all experiments to demonstrate that the proposed method does not rely on extensive hyperparameter tuning to achieve performance gains. We did not conduct a sensitivity analysis because our method uses a single configuration that generalizes effectively across all datasets and models.

5.2 Main Results and Analysis

Table 1 reports detailed forecasting performance across all datasets, prediction length, and model variants. Blue and red values indicate the best MSE and MAE for each task–model pair, respectively, and bold-underlined values mark the overall best result across all models for each task. Our approach ranks first in the majority of cases and outperforms baselines. Following [Wu et al., 2021, Zhou et al., 2021, Wu et al., 2022, Dao et al., 2022, Huang et al., 2022, Nie, 2022, Liu et al., 2023], scaling up the model projector is necessary for long-term forecasting. In contrast, our approach enables a single model to generate predictions of arbitrary length by concatenating AR rollout outputs. We denote this procedure as “(AR= k)” to indicate a k -step AR rollout.

Table 2 presents the results on additional datasets using the iTransformer and following the convention of [Liu et al., 2023], which does not report its variant performance on these benchmarks. The table illustrate the robustness of our method and performance gains across diverse domains.

Table 1: Forecasting performance on the Electricity, Traffic, and Weather datasets with fixed lookback length $S = 96$ and prediction lengths $T \in \{96, 192, 336, 720\}$. Task names are formatted by concatenating the dataset name + prediction length (e.g., “ECL_96”, “Traffic_720”). Baseline results are taken from the iTransformer paper. Prediction length under our method is extended to $(k \times T)$.

Task	Pred. Len.	iTransformer		iInformer		iFlowformer		iFlashformer	
		MSE	MAE	MSE	MAE	MSE	MAE	MSE	MAE
ECL_96	Baseline	0.148	0.240	0.190	0.286	0.183	0.267	0.178	0.265
	96 (AR=1)	0.141	0.239	0.131	0.232	0.141	0.241	0.142	0.241
	192 (AR=2)	0.163	0.260	0.154	0.254	0.167	0.266	0.169	0.267
	384 (AR=4)	0.194	0.288	0.184	0.282	0.207	0.301	0.206	0.300
	768 (AR=8)	0.238	0.324	0.229	0.320	0.263	0.345	0.257	0.340
ECL_192	Baseline	0.162	0.253	0.201	0.297	0.192	0.277	0.189	0.276
	192 (AR=1)	0.161	0.258	0.161	0.262	0.158	0.256	0.162	0.261
	384 (AR=2)	0.189	0.285	0.191	0.290	0.186	0.282	0.195	0.290
	768 (AR=4)	0.230	0.318	0.230	0.322	0.223	0.312	0.239	0.325
ECL_336	Baseline	0.178	0.269	0.218	0.315	0.210	0.295	0.207	0.294
	336 (AR=1)	0.177	0.275	0.187	0.288	0.178	0.276	0.184	0.282
	672 (AR=2)	0.209	0.302	0.230	0.323	0.213	0.306	0.221	0.312
ECL_720	Baseline	0.225	0.317	0.255	0.347	0.255	0.332	0.251	0.329
	720 (AR=1)	0.207	0.300	0.203	0.296	0.210	0.303	0.222	0.314
Traffic_96	Baseline	0.395	0.268	0.632	0.367	0.493	0.339	0.464	0.320
	96 (AR=1)	0.399	0.267	0.394	0.262	0.384	0.259	0.385	0.256
	192 (AR=2)	0.414	0.277	0.412	0.274	0.403	0.271	0.398	0.267
	384 (AR=4)	0.440	0.298	0.442	0.297	0.433	0.293	0.419	0.283
	768 (AR=8)	0.496	0.338	0.484	0.330	0.475	0.323	0.448	0.303
Traffic_192	Baseline	0.417	0.276	0.641	0.370	0.506	0.345	0.479	0.326
	192 (AR=1)	0.413	0.274	0.408	0.269	0.402	0.269	0.393	0.266
	384 (AR=2)	0.436	0.290	0.433	0.285	0.426	0.285	0.411	0.278
	768 (AR=4)	0.479	0.319	0.478	0.316	0.471	0.314	0.441	0.297
Traffic_336	Baseline	0.433	0.283	0.663	0.379	0.526	0.355	0.501	0.337
	336 (AR=1)	0.427	0.282	0.424	0.278	0.418	0.277	0.396	0.270
	672 (AR=2)	0.463	0.304	0.462	0.302	0.456	0.300	0.421	0.285
Traffic_720	Baseline	0.467	0.302	0.713	0.405	0.572	0.381	0.524	0.350
	720 (AR=1)	0.466	0.305	0.465	0.300	0.458	0.300	0.421	0.285
Weather_96	Baseline	0.174	0.214	0.180	0.251	0.183	0.223	0.177	0.218
	96 (AR=1)	0.160	0.210	0.147	0.201	0.161	0.211	0.162	0.212
	192 (AR=2)	0.203	0.235	0.190	0.242	0.203	0.250	0.203	0.250
	384 (AR=4)	0.262	0.294	0.248	0.286	0.259	0.292	0.260	0.293
Weather_192	Baseline	0.221	0.254	0.244	0.318	0.231	0.262	0.229	0.261
	192 (AR=1)	0.204	0.251	0.194	0.246	0.204	0.251	0.202	0.248
	384 (AR=2)	0.261	0.295	0.251	0.290	0.261	0.294	0.259	0.292
	768 (AR=4)	0.335	0.342	0.326	0.337	0.333	0.340	0.334	0.341
Weather_336	Baseline	0.278	0.296	0.282	0.343	0.286	0.301	0.283	0.300
	336 (AR=1)	0.251	0.286	0.246	0.286	0.249	0.285	0.250	0.287
	672 (AR=2)	0.320	0.331	0.318	0.332	0.317	0.330	0.319	0.332
Weather_720	Baseline	0.358	0.349	0.377	0.409	0.363	0.352	0.359	0.251
	720 (AR=1)	0.329	0.337	0.326	0.338	0.325	0.335	0.328	0.337

Table 2: Forecasting performance on additional benchmarks. “AR= k ” indicates k -step AR rollout from a short-horizon forecasting model.

Pred. Len.	PEMS04_96		PEMS07_96		Solar_96		Exchange_96		
	MSE	MAE	MSE	MAE	MSE	MAE	MSE	MAE	
96	Baseline (AR=1)	0.150 0.136	0.262 0.242	0.139 0.125	0.245 0.224	0.203 0.174	0.239 0.218	0.099 0.099	0.206 0.186
192	(AR=2)	0.172	0.274	0.162	0.255	0.226	0.256	0.274	0.306
288	(AR=3)	0.181	0.282	0.173	0.261	0.248	0.273	0.403	0.398
384	(AR=4)	0.196	0.293	0.186	0.270	0.267	0.287	0.478	0.441

5.2.1 Short-term Forecasting Improvements

Substantial gains are particularly evident in short-term forecasting. When the AR rollout step is set to 1, the model generates predictions in a short length manner. For example, on the Electricity dataset with a target prediction length of 96, iInformer MSE decreases from 0.190 to 0.131 (a 31% relative reduction) and becomes 12% lower than the iTransformer baseline of 0.148. Similarly, on the Traffic dataset with a target prediction length of 96, iFlashformer MSE decreases from 0.464 to 0.385 (an 18% relative reduction) while remaining lower than the iTransformer baseline. On the Weather dataset with a target prediction length of 96, iFlowformer MSE decreases from 0.183 to 0.161 (a 13% relative reduction).

5.2.2 SOTA Model Ranking Reversal

Under vanilla direct training, the base iTransformer consistently outperforms its variants—iInformer, iFlowformer, and iFlashformer—across datasets and horizons, establishing it as the strongest baseline among inverted Transformer models. In contrast, our proposed optimization strategy dramatically reshuffles this ordering. Variants that previously lagged now frequently achieve the best MSE and MAE values, often surpassing both the vanilla iTransformer and the AR-optimized base iTransformer. This reversal is consistent across short-, medium-, and long-term forecasting tasks. On Traffic, for example, optimized iFlashformer sets new SOTA results at multiple horizons (e.g., MSE 0.385 at prediction length 96, 0.393 at prediction length 192), while optimized iInformer and iFlowformer lead on select Electricity and Weather subtasks. The base iTransformer remains competitive but no longer dominates.

5.2.3 Error Accumulation in AR Rollout

Exploring the true trend of error accumulation in long-horizon forecasting is non-trivial. Experimental results are typically affected by two major factors: (1) differences in model scale (e.g., projector size or hidden dimension), and (2) extensive hyperparameters in training configuration (e.g., learning rate or batch size). In the past, poor performance of long-term forecasting has often been attributed to inherent limitations of the model architecture, when, in many cases, suboptimal training recipes are the dominant cause.

By generating predictions in the AR rollout mode, the model is fixed, allowing us to obtain a clear visualization of error accumulation behavior. As shown in Fig. 1, we observe that MSE increases roughly in proportion to the number of AR steps. This trend holds across nearly all model variants and datasets.

Note that the observed trend should not be interpreted as a scaling law [Kaplan et al., 2020] in the conventional sense. Unlike model scaling laws (where performance improves predictably with increases in parameter count or data volume), the degradation here arises purely from the compounding nature of AR generation with a fixed model size. The AR rollout strategy is simply an inference-time procedure for extending short-term predictions to long-term predictions; it does not involve any architectural scaling or model retraining.

6 Future Work

While the proposed optimization method enables flexible-length forecasting with a fixed model and delivers substantial performance gains across diverse datasets and model architectures, several important directions remain open for further investigation and refinement.

First, although our experiments and visualizations clearly reveal a nearly proportional (monotonic) relationship between error accumulation and the total prediction length (model projector length \times AR rollout steps), this trend has so far been characterized only empirically. A rigorous theoretical or quantitative analysis of this error propagation behavior is

in progress. Potential approaches include deriving bounds on the MSE/MAE for long-term forecasting under realistic assumptions about noise and bias amplification in the AR rollout iterations.

Subsequently, the core idea of our approach is to add a simple auxiliary penalty to discourage random-guess behavior in long forecasting chains. However, this approach leaves room for more sophisticated loss designs that use temporal causality for model training. As discussed in Section 2.2, the continuous-valued nature of time-series data makes RL difficult to apply to forecasting tasks. Our objective function is definitely only an RL-style loss, which may not effectively guide the model to achieve the highest rewards after training. Future work will explore lightweight hybrid RL ideas, such as proximal policy optimization [Schulman et al., 2017], to better avoid random-guess behavior in forecasting.

7 Conclusion

In this work, we introduced a novel loss function and training pipeline to address one of the most persistent challenges in modern time-series forecasting, AR rollout. Enabling a single fixed model to produce high-quality long-term predictions of arbitrary length without specialized architectural modifications or additional model retraining. Extensive experiments across diverse datasets demonstrate that our method improves the performance of iTransformer and its recent variants, achieving average MSE reductions exceeding 10% for both short- and long-term forecasting. Moreover, our proposed approach is preferable to directly training a long-horizon forecasting model: it enables effective reuse of a short-horizon forecasting model for long-term forecasting, surpassing specialized long-horizon forecasting models with larger-scale projectors. We believe this work opens promising avenues for time-series forecasting research.

References

Y Nie. A time series is worth 64words: Long-term forecasting with transformers. *arXiv preprint arXiv:2211.14730*, 2022.

Alexey Dosovitskiy. An image is worth 16x16 words: Transformers for image recognition at scale. *arXiv preprint arXiv:2010.11929*, 2020.

Yong Liu, Tengge Hu, Haoran Zhang, Haixu Wu, Shiyu Wang, Lintao Ma, and Mingsheng Long. itransformer: Inverted transformers are effective for time series forecasting. *arXiv preprint arXiv:2310.06625*, 2023.

Haixu Wu, Tengge Hu, Yong Liu, Hang Zhou, Jianmin Wang, and Mingsheng Long. Timesnet: Temporal 2d-variation modeling for general time series analysis. *arXiv preprint arXiv:2210.02186*, 2022.

Haoyi Zhou, Shanghang Zhang, Jieqi Peng, Shuai Zhang, Jianxin Li, Hui Xiong, and Wancai Zhang. Informer: Beyond efficient transformer for long sequence time-series forecasting. In *Proceedings of the AAAI conference on artificial intelligence*, volume 35, pages 11106–11115, 2021.

Zhaoyang Huang, Xiaoyu Shi, Chao Zhang, Qiang Wang, Ka Chun Cheung, Hongwei Qin, Jifeng Dai, and Hongsheng Li. Flowformer: A transformer architecture for optical flow. In *European conference on computer vision*, pages 668–685. Springer, 2022.

Tri Dao, Dan Fu, Stefano Ermon, Atri Rudra, and Christopher Ré. Flashattention: Fast and memory-efficient exact attention with io-awareness. *Advances in neural information processing systems*, 35:16344–16359, 2022.

Alec Radford, Karthik Narasimhan, Tim Salimans, Ilya Sutskever, et al. Improving language understanding by generative pre-training. 2018.

Massimiliano Marcellino, James H Stock, and Mark W Watson. A comparison of direct and iterated multistep ar methods for forecasting macroeconomic time series. *Journal of econometrics*, 135(1-2):499–526, 2006.

George EP Box, Gwilym M Jenkins, Gregory C Reinsel, and Greta M Ljung. *Time series analysis: forecasting and control*. John Wiley & Sons, 2015.

Aixin Liu, Bei Feng, Bing Xue, Bingxuan Wang, Bochao Wu, Chengda Lu, Chenggang Zhao, Chengqi Deng, Chenyu Zhang, Chong Ruan, et al. Deepseek-v3 technical report. *arXiv preprint arXiv:2412.19437*, 2024.

Fabian Gloeckle, Badr Youbi Idrissi, Baptiste Rozière, David Lopez-Paz, and Gabriel Synnaeve. Better & faster large language models via multi-token prediction. *arXiv preprint arXiv:2404.19737*, 2024.

Zheng Li, Jerry Cheng, and Huanying Helen Gu. Sequential policy gradient for adaptive hyperparameter optimization. *arXiv preprint arXiv:2506.15051*, 2025.

Haixu Wu, Jiehui Xu, Jianmin Wang, and Mingsheng Long. Autoformer: Decomposition transformers with auto-correlation for long-term series forecasting. *Advances in neural information processing systems*, 34:22419–22430, 2021.

Tian Zhou, Ziqing Ma, Qingsong Wen, Xue Wang, Liang Sun, and Rong Jin. Fedformer: Frequency enhanced decomposed transformer for long-term series forecasting. In *International conference on machine learning*, pages 27268–27286. PMLR, 2022.

Ashish Vaswani, Noam Shazeer, Niki Parmar, Jakob Uszkoreit, Llion Jones, Aidan N Gomez, Łukasz Kaiser, and Illia Polosukhin. Attention is all you need. *Advances in neural information processing systems*, 30, 2017.

Alec Radford, Jeffrey Wu, Rewon Child, David Luan, Dario Amodei, Ilya Sutskever, et al. Language models are unsupervised multitask learners. *OpenAI blog*, 1(8):9, 2019.

Victor Sanh, Albert Webson, Colin Raffel, Stephen H Bach, Lintang Sutawika, Zaid Alyafeai, Antoine Chaffin, Arnaud Stiegler, Teven Le Scao, Arun Raja, et al. Multitask prompted training enables zero-shot task generalization. *arXiv preprint arXiv:2110.08207*, 2021.

Alec Radford, Jong Wook Kim, Chris Hallacy, Aditya Ramesh, Gabriel Goh, Sandhini Agarwal, Girish Sastry, Amanda Askell, Pamela Mishkin, Jack Clark, et al. Learning transferable visual models from natural language supervision. In *International conference on machine learning*, pages 8748–8763. PMLR, 2021.

Keyu Tian, Yi Jiang, Zehuan Yuan, Bingyue Peng, and Liwei Wang. Visual autoregressive modeling: Scalable image generation via next-scale prediction. *Advances in neural information processing systems*, 37:84839–84865, 2024.

Stephen Boyd and Lieven Vandenberghe. *Convex optimization*. Cambridge university press, 2004.

Xinlei Chen and Kaiming He. Exploring simple siamese representation learning. In *Proceedings of the IEEE/CVF conference on computer vision and pattern recognition*, pages 15750–15758, 2021.

Richard S Sutton, David McAllester, Satinder Singh, and Yishay Mansour. Policy gradient methods for reinforcement learning with function approximation. *Advances in neural information processing systems*, 12, 1999.

Jared Kaplan, Sam McCandlish, Tom Henighan, Tom B Brown, Benjamin Chess, Rewon Child, Scott Gray, Alec Radford, Jeffrey Wu, and Dario Amodei. Scaling laws for neural language models. *arXiv preprint arXiv:2001.08361*, 2020.

John Schulman, Filip Wolski, Prafulla Dhariwal, Alec Radford, and Oleg Klimov. Proximal policy optimization algorithms. *arXiv preprint arXiv:1707.06347*, 2017.